

# EXPERIMENTAL ANALYSIS OF TIMBER-CONCRETE COMPOSITES WITH INNOVATIVE FRP CONNECTORS

Songnan Li<sup>1</sup>, S. Ali Hadigheh<sup>2</sup>

**ABSTRACT:** This study aims to investigate the structural behaviour of timber-concrete composite (TCC) connections with innovative shear connectors made of fibre-reinforced polymer (FRP) materials. A total of 18 push-out tests are conducted on six groups of symmetric TCC joints with conventional and FRP composite connectors. The conventional connectors are steel screws and perforated steel plates (PSP). The FRP connectors introduced in this study include T-shaped plates fabricated from bidirectional FRP mats and helically wrapped FRP rods. Both carbon FRP (CFRP) and glass FRP (GFRP) materials are employed to investigate the effect of composite material type on the structural performance of the connectors. The load-slip behaviour, maximum load-carrying capacity, stiffness and failure modes are evaluated in detail. The outcomes of the shear tests demonstrate that specimens with GFRP rods exhibit the highest load-carrying capacity and serviceability stiffness among all tested specimens. In addition, connections utilising T-shaped GFRP plates achieve the second highest maximum load-bearing capacity and stiffness. Although slightly lower in performance than the GFRP connectors, T-shaped CFRP plates and CFRP rods also showed enhanced load-carrying capacity and stiffness compared to the conventional SFS screws connectors.

**KEYWORDS:** Timber concrete composite, Fibre-reinforced polymer, Steel, Load-carrying capacity, Stiffness

## 1 – INTRODUCTION

In recent years, engineering wood products (EWPs) are increasingly being utilised as substitutes for conventional steel and concrete in a variety of construction projects to minimise environmental impacts. EWPs used in construction include cross-laminated timber (CLT), glue-laminated timber (GLT), and laminated veneer lumber (LVL). CLT is particularly notable for its orthotropic layer orientation, where each layer is positioned perpendicular to the adjacent ones. This unique configuration enhances both in-plane and out-of-plane strength and stiffness. However, despite the construction benefits provided by the lighter weight of timber materials, this can lead to reduced stiffness, which may impact structural performance in terms of serviceability and ultimate limit states. To mitigate this issue, timber is combined with concrete to create a timber-concrete composite (TCC) system [1].

TCC structures have gained popularity due to their advantages, such as high strength-to-weight ratio, low carbon emissions, and ease of construction. In TCC structures, the connections play a crucial role in transferring the shear force between two sections and improving the structural integrity. Extensive studies have been conducted to investigate the performance of various types of connections. The use of SFS screws in TCC improves the serviceability slip modulus, though they

exhibit lower ductility manifested by sudden and significant loss of the load-carrying capacity after the peak [2]. Innovative approaches, such as combining perforated steel plate (PSP) with steel reinforcement bars as connectors, have achieved very high load-carrying capacities with minimal deformation, albeit with construction challenges [3]. Research by Hadigheh et al. [4] explored the use of carbon fibre-reinforced polymer (CFRP) connectors in TCC beams, with the CFRP rods demonstrating the highest ultimate load, bending stiffness, and ductility compared to SFS screw and PSP connections. However, the CFRP plates lacked sufficient bond with concrete and failed due to debonding. Despite these findings, research on the use of FRP materials as connectors in TCC systems remains limited.

In this research, innovative T-shaped FRP plate connections made from CFRP, and glass fibre-reinforced polymer (GFRP) composite are introduced. Push-out tests are conducted to examine the shear behaviour of FRP connections, including stiffness, load-carrying capacity, and failure mechanisms, and to compare their performance against conventional steel connections.

## 2 – EXPERIMENTAL PROGRAM

CLT panel was placed between two concrete blocks to form a symmetric specimen. The shear connectors used in the tests included SFS, CFRP rods (CR) and GFRP

<sup>1</sup> Songnan Li, School of Civil Engineering, The University of Sydney, Sydney, Australia, [songnan.li@sydney.edu.au](mailto:songnan.li@sydney.edu.au)

<sup>2</sup> S. Ali Hadigheh, School of Civil Engineering, The University of Sydney, Sydney, Australia, [ali.hadigheh@sydney.edu.au](mailto:ali.hadigheh@sydney.edu.au)

rods (GR), PSP, and T-shaped CFRP plates (CP) and GFRP plates (GP). The T-shaped FRP plates were fabricated by the wet-layup method. The PSP, FRP plates and FRP rods were installed into timber slots and holes by using Sikadur-330 two-part epoxy. The design of the spacing, edge distance and embedment length of the connection are based on Eurocode 5 [5] and a previous study [4]. To ensure a valid comparison between connectors made of different materials, the dimensions of the connectors were determined based on the equivalent axial stiffness.

## 2.1 MATERIAL PROPERTIES

CLT panels used in this study were made from Australian radiata pine, with cross-sectional dimensions of 150 × 500 mm<sup>2</sup> and a thickness of 240 mm. Given the significant influence of the outer layer on the structural performance, it was assigned a higher grade than the inner layers. The panels consist of seven layers, with the outermost layers being 32.5 mm thick and the inner five layers being 35 mm thick. The elastic modulus and specific strength properties of the CLT are detailed in **Table 1**.

In this study, C40 concrete with a maximum aggregate size of 20 mm was used. To evaluate its compressive strength, four concrete cylinders measuring 150 mm × 300 mm were tested on the day of the push-out test, resulting in an average compressive strength of 42.6 MPa.

The SFS VB-48-7.5 screws were selected for their robust design, making them ideal for securing heavy and large components. These screws have deep, continuous threads

along half-length, optimising timber embedment, and a hexagonal screw head that enhances withdrawal strength from concrete. The nominal diameter of the SFS screw is 7.5 mm, and its tensile strength is 17 kN.

CR and GR were manufactured using the pultrusion process, which bonds unidirectional fibres into a solid, uniform rod. Both CR and GR feature a helically wrapped profile to improve their embedment strength with concrete. The diameter of CR and GR were determined to be 8 mm and 13 mm, respectively, by adjusting their axial stiffness (EA) to match that of the SFS screw.

For plate connections, PSPs were used as shear connectors because of their high ductility. The holes in the PSPs improve the interaction between the concrete and the connector by allowing cement and fine aggregates to penetrate, thereby increasing the withdrawal strength. The dimensions of PSPs are 80 × 150 × 2 mm<sup>3</sup>, and the tensile strength is 35.6 kN.

As the counterparts of PSP, customised CP and GP were produced using a wet lay-up technique in the laboratory using Kinetix two-part epoxy [6]. To overcome the challenges of creating T-shaped plates, two L-shaped FRP plates were made and then bonded back-to-back with Sikadur-330 epoxy to form a T-shaped plate. This method facilitated the production of the desired T-shaped configuration. The tensile strength of CP and GP was tested according to the D3039/D3039M-17 [7], with the results shown in **Figure 1**. For installing these connections, except for the SFS screws, the two-part

**Table 1:** Material properties of CLT

	External lamella	Internal lamella
Mean density, $\rho$	500 kg/m <sup>3</sup>	480 kg/m <sup>3</sup>
Elastic modulus (parallel), $E_0$	10,000 MPa	6,000 MPa
Bending (parallel), $f_{b,0}$	17 MPa	10 MPa
Compression (parallel), $f_{c,0}$	18 MPa	15 MPa
Compression (perpendicular), $f_{c,90}$	10 MPa	8.9 MPa
Tension (parallel), $f_{t,0}$	7.7 MPa	4 MPa
Shear (parallel), $f_{s,0}$	3.8 MPa	3.8 MPa
Shear modulus, $G_0$	670 MPa	400 MPa

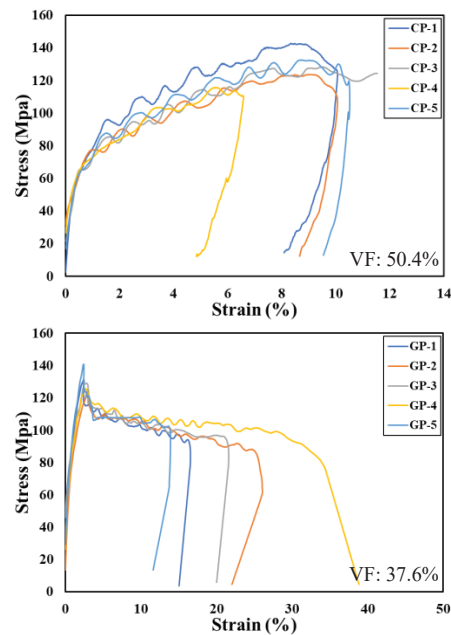


**Figure 1:** Stress-strain curve of CP and GP

**Table 2: Material properties of FRP rods and epoxy**

Parameters	Value	Parameters	Value
<b>CFRP Rod</b>			
Nominal diameter (mm)	8	Tensile strength (MPa)	2,378
Length (mm)	160	Elastic modulus (GPa)	143
Elongation (%)	1.4		
<b>GFRP Rod</b>			
Nominal diameter (mm)	13	Tensile strength (MPa)	972
Length (mm)	160	Elastic modulus (GPa)	60
Elongation (%)	1.6		
<b>Sikadur-330 epoxy</b>			
Tensile strength (MPa)	30	Elastic modulus in tension (MPa)	4,500
Compression strength (MPa)	80	Tensile elongation (%)	0.9
Density (g/cm <sup>3</sup> )	1.3		
<b>Kinetix R240 resin</b>			
Tensile strength (MPa)	83.3	Elastic modulus in tension (MPa)	3,650
Compression strength (MPa)	98	Tensile elongation (%)	9.8
Density (g/cm <sup>3</sup> )	1.1		

epoxy Sikadur-330 was injected into the pre-drilled holes and slots in the timber. The material properties of FRP rods and epoxy are shown in **Table 2**.

**2.2 DESIGN OF SPECIMENS**

The specimens with SFS and FRP rods were arranged in two vertical cross pairs on each side. This configuration places two connectors in tension and two in compression, optimising the structural interactions of the connections. The configurations of TCC with SFS and FRP rods are

shown in **Figure 2a**. For the plate connections, the design configuration included one connection at each shear plane, as indicated in **Figure 2b**. The embedment depth within the timber is set at 50 mm, ensuring a strong bond between the connection and the timber.

**2.3 EXPERIMENTAL SETUP**

A total of 18 push-out tests were carried out by a DARTEC hydraulic loading machine to assess the shear performance of the connectors, the details of the specimen are listed in **Table 3**. To ensure stability and prevent any movement during testing, the specimens were securely mounted on a steel test frame as shown in **Figure 3a**. The tests followed the loading protocol in

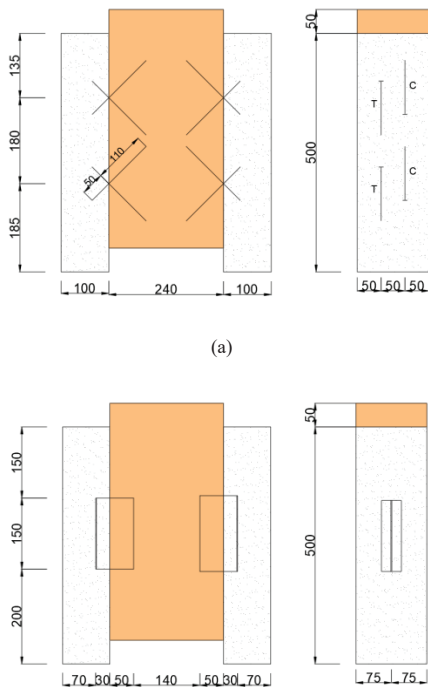


**Figure 2: Configurations of: (a) SFS, CR, GR (b) PSP, CP, GP.**

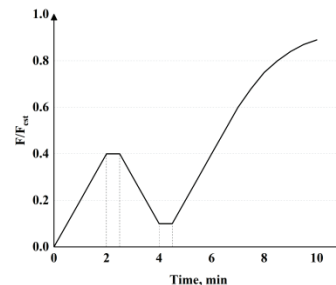
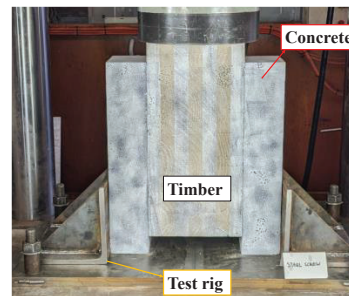


**Figure 3: (a) Test setup (b) loading procedure [8]**

**Table 3: Details of specimen**

Specimens	Number of specimens	Connection
SFS	3	SFS screw
CR	3	CFRP rod
GR	3	GFRP rod
PSP	3	Perforated steel plate
CP	3	T-shaped CFRP plate
GP	3	T-shaped GFRP plate

accordance with EN 26891:1991 [8], initially loaded up to 40% of the  $F_{est}$  (estimated maximum load), held for 30s, then unloaded to 10% of  $F_{est}$  and maintained for 30s, finally, and finally the specimen was loaded until failure, as indicated in **Figure 3b**.

### 3 – RESULTS AND DISCUSSION

#### 3.1 LOAD-SLIP RESPONSE

The load-slip response of the specimens is illustrated in **Figure 4**. Consistent responses were observed within each connection, except for the PSP-3 sample, which was excluded from the analysis due to concrete pouring errors. All connections experienced four stages during testing: (i) linear elastic stage, (ii) elastic-plastic stage, (iii) post-peak decline, and (iv) residual plateau at failure. The PSP samples displayed minor drops and re-rise behaviour after reaching the first peak. This slight drop is attributed

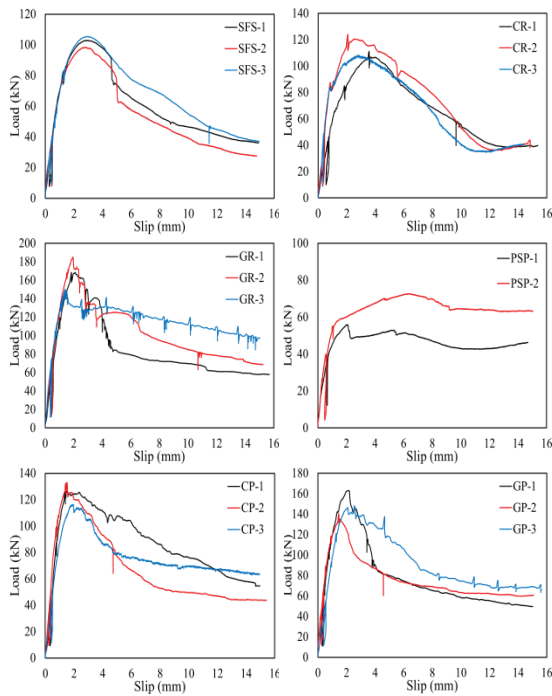


**Figure 4: Load-slip response curves**

to the lower load-carrying capacity of PSP connections compared to other connections, while the resurgence is due to the residual strength of the connector. The other connections showed an abrupt drop after reaching peak load due to connection fractures and concrete cracking.

The maximum load-carrying capacity, serviceability stiffness and ductility are shown in **Table 4**. According to EN 26891:1991 [8], the serviceability stiffness of the connections can be calculated using (1).

$$k_{04} = (0.4F_{est} - 0.1F_{est}) / (v_{04} - v_{01}) \quad (1)$$

Where,  $v_{01}$  and  $v_{04}$  represent the slips corresponding to the 10% and 40% peak load, respectively. The ductility of each connection was obtained from (2) based on [9].

$$D = V_u / V_y \quad (2)$$

Where  $V_u$  and  $V_y$  represent the slip correspond to the ultimate and yield point. Among all the connections, the GR exhibited the highest average peak load and serviceability stiffness at 168.0 kN and 144.0 kN/mm, respectively. This performance suggests a robust composite action between timber and concrete components, critical for high-load applications. Following this, the GP exhibited a maximum load capacity of 150.4 kN. The stiffness of the GP is close to the GR because the flange of the plate provided an additional bond between the connection and concrete. However, GP exhibited a sharp decline in post-peak behaviour, highlighting a limitation in ductility. In contrast, CP demonstrates a balance between the load-carrying capacity and ductility, achieving an average peak load of 125.3 kN and displaying a more gradual decline after the peak load, which indicates enhanced ductile behaviour. CR demonstrated a slightly lower maximum load and stiffness compared to CP. The SFS and PSP demonstrated lower peak load due to the limited strength of the material, with a maximum load of 102.3 kN and 64.3 kN, respectively. Their lower serviceability stiffness was evident from the load-slip curves. Notably, despite its lowest load capacity, the PSP demonstrated the highest ductility among all the specimens. This performance is attributed to the ductile behaviour of the steel material and the improved load redistribution, facilitated by the bonding of aggregates filling the holes in the plate.

#### 3.2 FAILURE MODES

The failure modes observed in the TCC joints with SFS showed a consistent pattern. No visible cracks appeared on the surface of either the timber or concrete, but a clear separation between these two components was evident. Upon removing the samples from the test rig, it was noted that the screws had failed to maintain their connection between the timber and concrete. Screws had partially pulled out of the timber, causing the surrounding timber to crush due to the withdrawal force.

**Table 4:** Experimental results for push-out tests on TCC joints

	Specimen	Peak load			$k_{04}$ (kN/mm)			Ductility	
		$F_{max}$ (kN)	Mean(kN)	COV	$k_{04}$	Mean	COV	$V_u/V_y$	Mean
Screw/Rod connections	SFS-1	102.9			83.4			5.7	
	SFS-2	98.5	102.3	2.8%	70.3	77.6	7.0%	3.9	4.8
	SFS-3	105.5			79.2			4.8	
	CR-1	111.2			60.4			4.3	
	CR-2	124.1	114.6	6.0%	107.9	110.8	38.3%	5.7	6.2
	CR-3	108.4			164.2			8.5	
	GR-1	168.5			124.8			3.5	
	GR-2	185.2	168.0	8.5%	141.4	144.0	11.7%	2.3	3.5
	GR-3	150.3			165.8			4.8	
Plate connections	PSP-1	56.0			63.9			13.6	
	PSP-2	72.6	64.3	12.9%	82.9	73.4	12.9%	14.2	13.9
	CP-1	126.4			114.9			6.5	
	CP-2	133.0	125.3	5.4%	149.5	124.5	14.3%	4.7	5.0
	CP-3	116.5			109.2			3.7	
	GP-1	163.0			168.7			2.8	
	GP-2	140.3	150.4	6.3%	138.0	143.1	13.4%	3.5	3.8
	GP-3	147.8			122.5			5.2	

Plastic hinge occurred at the portion of the screw in the tension side within the timber, as illustrated in **Figure 5**. The SFS on the compression side was sheared off at the interface of the timber and concrete.

The CR samples showed a minor separation during testing, which indicated a higher composite action compared to SFS connections. A minor crack was observed on the surface of the concrete. After a closer examination, there was no debonding between CR and timber, indicating that adhesion failure did not play a role in the sample failure. Similar to SFS connections, the CR connection on the compression side was also sheared off at the interface of timber and concrete component.

GR was selected with a larger diameter because of its lower elastic modulus. Therefore, the contact area between GR and concrete is greater than CR. During testing, a large crack extended from the interior of the concrete to its surface in the GR specimens. After investigating the interior of the GR specimen, there was no timber crushing or debonding. Additionally, the GR on the compression side was also sheared off at the concrete-timber interface. This consistent failure pattern across different materials highlights the critical stress points at the material interface in composite structures.

PSP samples were easily separated after removing from the test rig. This was likely due to the fact that large aggregates in the concrete could not enter into the holes on the plate to significantly enhance withdrawal strength. Cracks in the concrete propagated from the contact points between the concrete and the PSP, as shown in **Figure 5**. This suggests that the localised stress from the connection exceeded the concrete's bearing capacity. Additionally, it was observed that the connection yielded, and the timber did not split after failure.

Similar failure modes occurred in CP and GP specimens. During testing, large cracks propagated to the concrete surface. The  $\pm 45^\circ$  orientation of the fibres resulted in delamination at a 45-degree angle across both the web and flange of the plate. The curvature at the junction between the flange and the web on the T-shaped plate effectively mitigated stress concentration at this point. There was no noticeable debonding between the connector and timber or within the interface between the two L-shaped plates. The FRP plate maintained its T-shape, and most parts remained uncracked, demonstrating the desired behaviour while maintaining structural integrity.

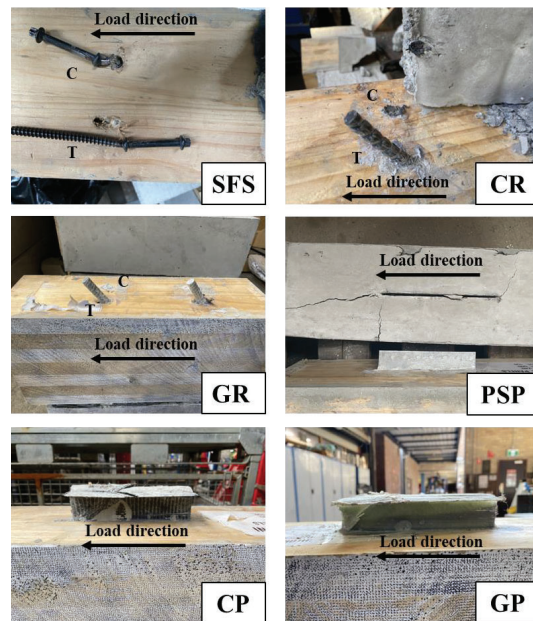


**Figure 5:** Failure modes

## 4 – CONCLUSIONS

This study experimentally evaluated the shear performance of new types of shear connectors fabricated from FRP materials in TCC connections. Push-out tests were performed to examine the load-slip behaviour, serviceability stiffness, ductility, and failure mechanisms of the samples. By comparing the shear performance of FRP connections to conventional steel connections, the benefits of FRP connections have been evaluated.

The main conclusions of this study are:

- GR and GP outperform all other connectors in terms of load-carrying capacity and serviceability stiffness.
- Connections made from CFRP composite were less effective than their GFRP counterparts, they still exceeded the performance of the conventional steel connectors.
- CR and CP show higher ductility among all FRP connectors.

Future research should include conducting beam tests to assess the bending performance of these FRP connections. Such tests will provide a more detailed understanding of the capabilities and limitations of these new connections in beam applications.

## ACKNOWLEDGEMENT

The authors would like to thank the School of Civil Engineering at the University of Sydney for supporting this project. The second author would like to acknowledge the support he received from the Australian Government through the Australian Research Council's Discovery Early Career Researcher Award (DECRA) fellowship scheme (project DE200100406). The authors would also like to thank XLAM, Pultron Composite, and Rothoblaas for providing the CLT, GFRP rods, steel screws and perforated plates for this project.

## REFERENCES

- [1] CEN/TS 19103:2001, Eurocode 5: Design of Timber Structures - Structural design of timber-concrete composite structures - Common rules and rules for buildings. Brussels, Belgium, 2021.
- [2] Khorsandnia N, Valipour HR, Crews K. Experimental and analytical investigation of short-term behaviour of LVL-concrete composite connections and beams. *Construction and Building Materials*. 2012;37:229-38.
- [3] Suárez-Riestra F, Estévez-Cimadevila J, Martín-Gutiérrez E, Otero-Chans D. Perforated shear+ reinforcement bar connectors in a timber-concrete composite solution. Analytical and numerical approach. *Composites Part B: Engineering*. 2019;156:138-47.

[4] Hadigheh S, McDougall R, Wiseman C, Reid L. Evaluation of composite action in cross laminated timber-concrete composite beams with CFRP reinforcing bar and plate connectors using Digital Image Correlation (DIC). *Engineering Structures*. 2021;232:111791.

[5] Eurocode 5: Design of Timber Structures—Part 1–2: General—Structural Fire Design. Brussels, Belgium, 2004.

[6] Hadigheh SA, Gravina R. Generalization of the interface law for different FRP processing techniques in FRP-to-concrete bonded interfaces. *Composites Part B: Engineering*. 2016;91:399-407.

[7] D3039/D3039M-17 Standard Test Method for Tensile Properties of Polymer Matrix Composite Materials. 2017.

[8] EN 26891:1991, Timber structures — Joints made with mechanical fasteners — General principles for the determination of strength and deformation characteristics. Brussels, Belgium, 1991.

[9] EN 12512:2001, Timber structures - Test methods - Cyclic testing of joints made with mechanical fasteners. Brussels, Belgium, 2001.